ISSN 0023-1584, Kinetics and Catalysis, 2010, Vol. 51, No. 4, pp. 475–484. © Pleiades Publishing, Ltd., 2010.
Original Russian Text © N.M. Rubtsov, B.S. Seplyarskii, G.I. Tsvetkov, V.I. Chernysh, 2010, published in Kinetika i Kataliz, 2010, Vol. 51, No. 4, pp. 499–509.

High-Speed Color Cinematography of Chain Self-Ignition in the Hydrogen, Methane, and Isobutylene Oxidation Reactions

N. M. Rubtsov, B. S. Seplyarskii, G. I. Tsvetkov, and V. I. Chernysh

Institute of Structural Macrokinetics and Materials Research Problems, Russian Academy of Sciences, Chernogolovka, Moscow oblast, 142432 Russia

e-mail: nmrubtss@mtu-net.ru

Received June 17, 2009

Abstract—The spatial development of chain self-ignition in the oxidation of stoichiometric mixtures of hydrogen, methane, and isobutylene with oxygen at total pressures of 10–100 Torr and $T = 750$–1000 K has been investigated by high-speed color cinematography. The spatial development of the chain process is governed by the properties of the reactor surface and by the heating time of the combustible mixture. A numerical simulation of the process has been carried out.

DOI: 10.1134/S0023158410040038

Data concerning the spatial development of the self-ignition of combustible gases in contact with a hot surface are of marked interest in the context of use of hydrocarbons and potential use of hydrogen as fuels for engines and power plants. Hydrogen fuel is environmentally friendly since the product of its combustion is water. One of the main factors hampering the progress of hydrogen energy engineering is the excessively high combustibility and explosibility of hydrogen in air: the combustion of hydrogen–air mixture can evolve into detonation in a wide range of hydrogen concentrations.

The information that has been reported on the spatial development of the self-ignition of combustible gases is scanty. The development of silane self-ignition in oxygen over the 4–500 Torr pressure range at initial temperatures of 300–400 K was studied by high-speed schlieren cinematography [1]. It was demonstrated that self-ignition begins on the reactor surface and involves adsorbed reactive species.

Hydrogen self-ignition at low pressures (~1 Torr) near the lower self-ignition limit is believed to be uniform throughout the reactor volume [2]. However, it should be expected that the heating time required for the complete temperature equalization over the reactor diameter will lengthen with an increasing total pressure of the combustible mixture. This will increase the probability of the self-ignition of the mixture near the reactor surface. Therefore, the undistributed self-ignition problem may transform into the problem of the ignition of a combustible mixture by a hot surface [3–5]. In this case, it is crucial to take into account the heating time because this will lead to a radically different dependence of the ignition delay on the characteristic size of the system.

Another factor in the uniformity of self-ignition is the properties of the reactor surface. Platinum black is known to exert a promoting effect on hydrogen oxidation [6]. It was demonstrated that the promoting effect of the surface material is due to the heterogeneous propagation of reaction chains [7]. The occurrence of heterogeneous chain propagation reactions also raises the probability of the combustible mixture self-igniting near the surface.

Here, we present a high-speed color cinematographic study of the spatial development of chain self-ignition in the oxidation reactions of stoichiometric hydrogen-, methane-, and isobutylene-oxygen mixtures. We also demonstrate qualitatively by means of numerical simulation how the spatial development of self-ignition depends on the ratio between the heating time and the characteristic time of the chemical reaction, on the character of heterogeneous chain termination, and on the occurrence of surface reactions.

EXPERIMENTAL

Experiments were performed using a static vacuum technique [8]. The reactor was a furnace-heated quartz cylinder 3.6 cm in diameter and 25 cm in length. The furnace temperature was set using a KVA-501 temperature regulator with an accuracy of ±0.5 K. The reactor had an optical quartz window at one end. Preblended stoichiometric mixtures of hydrogen, natural gas (NG), and isobutylene (i-C_4H_8) with oxygen were examined.

In the event of self-ignition, we recorded the emission from the electronically excited OH^* ($A^2\Sigma^+$) radicals at $\lambda = 306$ nm using an interference filter ($\Delta\lambda = 25$ nm) and an FEU-71 photomultiplier. The signal from the photomultiplier was directed to one of the

inputs of an S9-16 dual-trace memory oscilloscope operating in the leading mode. The mixture admission valve had a thin blackened organic-glass blade. When the valve was closed, this blade shuttered the light coming from the emitter to the photodiode. As the valve was being opened, admitting the combustible mixture into the reactor, the blade shifted and the signal from the photodiode arrived at the synchronization input of the S9-16 oscilloscope. This technique enabled us to measure ignition delays as the time interval between the mixture admission point and the ignition chemiluminescence peak with a high degree of accuracy.

The lower limit pressure P_1 was determined by the bleed-off method [9]. The ignition of $2H_2 + O_2$ mixtures was studied in a quartz reactor whose surface was pretreated with HF and in a quartz reactor whose walls were coated with magnesium oxide. The ignition of NG + $2O_2$ and i-C_4H_8 + $6O_2$ mixtures was studied in a quartz reactor whose surface was pretreated with HF. The total pressure (P_0) was varied between 10 and 100 Torr. The furnace temperature was varied in the 750–1000 K range. Between runs, the reactor was vacuumized to 10^{-2} Torr with a 2NVR-5D fore pump. Pressure was measured with a VDG-1 gas-discharge manometer and a VIT-2 vacuometer. According to gas chromatography data, NG contained 98% methane and 2% (propane + butane); H_2, O_2, and i-C_4H_8 were reagent grade.

The visible light emitted by self-igniting gas mixtures was filmed on a Casio Exilim F1 Pro camera (frame frequency of 1200 s^{-1}). The signal from the camera was input in a computer. The time point to start filming was determined from preliminary self-ignition delay data.

RESULTS AND DISCUSSION

Figure 1 shows a sequence of video images (frame frequency of 1200 s^{-1}) of the spatial development of ignition in the $2H_2 + O_2$ mixture over a quartz surface (under kinetically controlled chain termination [2]). It can be seen in Figs. 1a and 1b that the spatial uniformity of self-ignition is governed by the properties of the surface. In the case of the surface washed with HF before measurements, hydrogen ignition in the first run takes place near the surface (Fig. 1a). After four runs, the self-ignition process moves from the surface to the gas bulk (Fig. 1b). The flash over the "fresh" surface differs in color from the flash observed after a few self-ignition runs. This indicates a difference between the spectral compositions of chemiluminescence in these two cases. Under the experimental conditions specified in Figs. 1a and 1b, the self-ignition delay time is $\tau \sim 0.3$ s. Note that the τ value thus measured is the upper limit of the true ignition delay [2].

The observed ignition delay includes the time taken for the admission of the combustible mixture into the reactor. The gas admission time for the same setup with the same reactor was measured directly in our earlier study [8]. This time was 0.3–0.4 s [8, Fig. 1]. Thus, the gas admission time is comparable with the ignition delay for the $2H_2 + O_2$ mixture without an inhibitor (Figs. 1a, 1b). However, the surface of the reactor is so active that the combustible mixture burns up just on this surface. When the ignition delay is longer than 4 s, both the gas admission time and the heating time can be neglected as much smaller values. Since this work deals with the qualitative effects of the determining parameters on the spatial development of ignition, taking into account the gas admission time cannot cause qualitative changes in the results.

According to our estimates, the calculated mixture heating time can be either longer or shorter than the ignition delay, depending on whether the thermal diffusivity at the initial temperature or that at the wall temperature is used in the calculation. We will illustrate this point by direct calculations, neglecting radiant heating. The heating time for a mixture in an infinitely long cylindrical vessel under Dirichlet boundary conditions can be taken to be $t_h = r^2/\alpha$, where r is the radius of the vessel and α is thermal diffusivity [4]. Substituting the α values corresponding to the initial temperature ($\alpha = 13.8$ cm^2/s) and wall temperature ($\alpha = 37.8$ cm^2/s) into this formula, we obtain $t_h = 0.25$ s for $T = 300$ K and $t_h = 0.085$ s for $T = 823$ K. In our calculations, we set the thermal diffusivity to be equal to the hydrogen diffusion coefficient. For the stoichiometric H_2–O_2 mixture, the hydrogen diffusion coefficient and, accordingly, α are close to 1 cm^2/s at 293 K and 1 atm [2]. Hence, $\alpha \approx 75$ cm^2/s under the experimental conditions specified in Figs. 1a and 1b ($P_0 = 55$ Torr, $T = 823$ K). Therefore, the experimental conditions indicated in Figs. 1a and 1b fall in the region of high parametric sensitivity to changes in the determining parameters, even if these changes are so small that they have no effect on the ignition delay. This is the reason why, under the experimental conditions specified in Fig. 1b, the changes in the properties of the surface (apparently, its deactivation) as a result of ignition and combustion runs bring the ignition process from the surface to the bulk.

Note that raising the total pressure of the combustible mixture to 100 Torr causes the surface ignition of the mixture both in the fresh reactor and in the reactor treated with flashes of light. The ignition and burning times shorten, and the flashes themselves begin to be accompanied by clicks. The cause of this effect of the total pressure on ignition is that, on the one hand, an increasing pressure increases the thermal diffusivity and, on the other hand, it speeds up the oxidation reaction at the same wall temperature. This changes the ratio between the gas heating time (which is generally inversely proportional to thermal diffusivity) and the oxidation time. As a consequence, the mixture ignites even in the reactor treated with flashes of light.

In order to ensure the uniform heating of the combustible mixture before its ignition, we used 4% i-C_4H_8

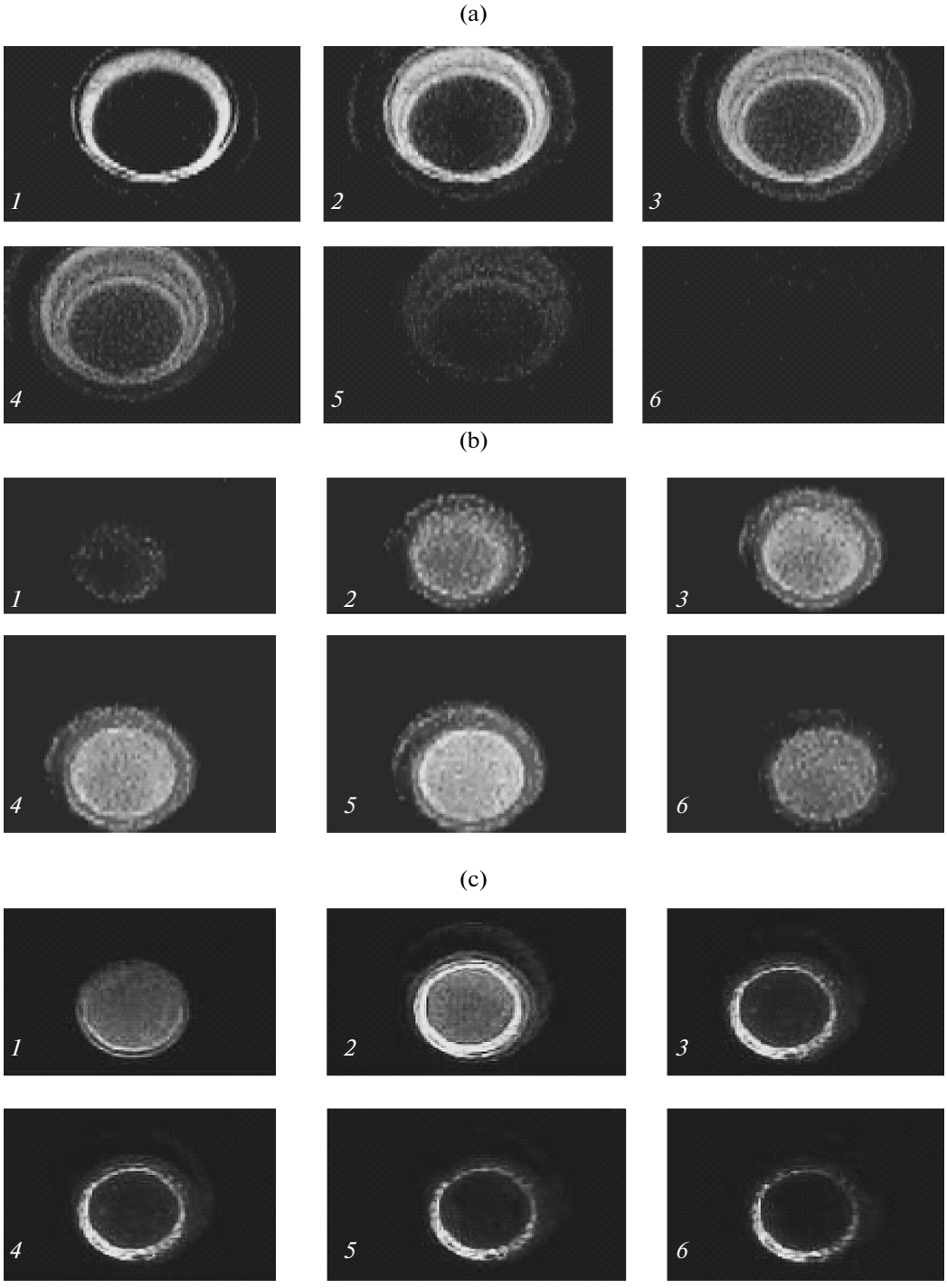

Fig. 1. Spatial development of self-ignition in the $2H_2 + O_2$ mixture over a quartz surface: (a) $P_0 = 55$ Torr, $T_0 = 823$ K, fresh surface treated with HF, first run; (b) $P_0 = 55$ Torr, $T_0 = 823$ K, fifth run; (c) 4% i-C_4H_8, $P_0 = 70$ Torr, $T_0 = 883$ K. The numerals in the frames are their sequential numbers from the onset of light emission.

as the inhibitor, which markedly lengthens the ignition delay [10]. Under the conditions specified in Fig. 1c, the ignition delay is 9 s. According to our estimates, this time is sufficient for the combustible mixture to heat uniformly throughout the reactor volume. The light emission from the bulk of the mixture in this case is due in part to the $C_2^{\bullet}$ radicals ($A^3P_g - X^3P_u$) [9], which result from the oxidation of the hydrocarbon admixture.

Note that hydrogen combustion over a magnesium oxide surface (in the diffusion-controlled region of

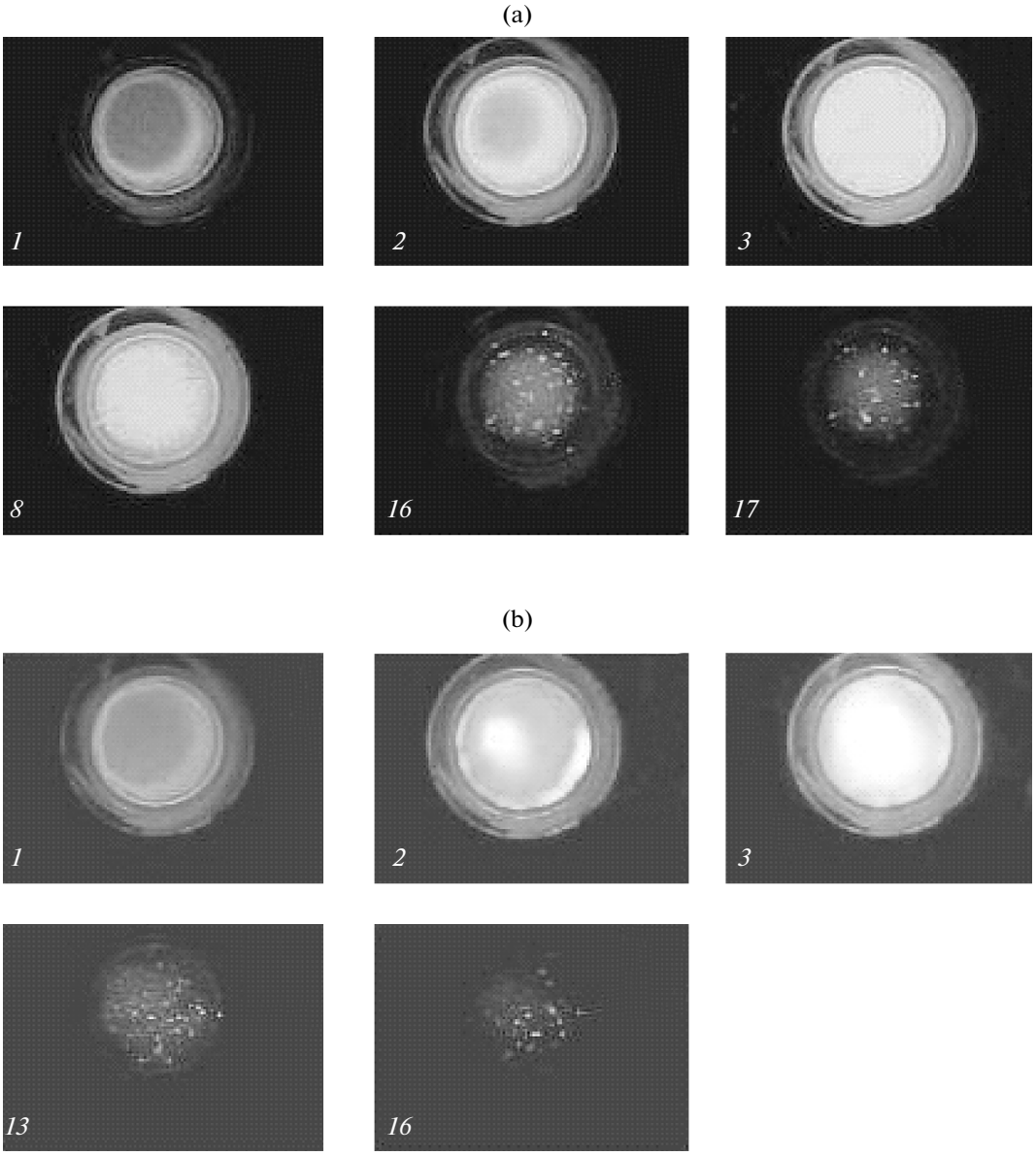

Fig. 2. Spatial development of self-ignition in gas mixtures over a quartz surface treated with HF: (a) NG + $2O_2$, $P_0 = 78$ Torr, $T_0 = 993$ K; (b) i-$C_4H_8 + 6O_2$, $P_0 = 56$ Torr, $T_0 = 993$ K, 557-nm optical filter selecting the emission band of the $C_2^{\bullet}$ radical (A^3P_g–X^3P_u, $\nu = 0$–1). The numerals in the frames are their sequential numbers from the onset of light emission.

chain termination) in the 20–40 Torr pressure range at 900 K develops uniformly throughout the reactor volume.

Figures 2a and 2b present a sequence of video images (1200 frames per second) of the spatial development of self-ignition in NG + $2O_2$ and i-$C_4H_8 + 6O_2$ mixtures over a quartz surface. The self-ignition pressures here are near the methane self-ignition pressure [11], and the ignition delay is ~30 s. Estimates demonstrate that, during the ignition delay, the combustible mixture heats uniformly up to the wall temperature. The self-ignition process begins on the reactor surface and then propagates into the bulk (Figs. 2a, 2b). Therefore, the NG and isobutylene reactions on the quartz surface are catalytic.

The above results were interpreted qualitatively using simulation of hydrogen oxidation, whose kinetic mechanism can be considered to be known for certain [2, 9]. In this simulation, we investigated the effects of the ratio between the heating time and the characteristic time of the chemical reaction, the character of chain termination (kinetically controlled versus diffusion-controlled), and the occurrence of surface reactions on the spatial development of self-ignition in a confined channel. Limited to qualitative consideration, we ignored radiant heating.

The reduced kinetic mechanism of hydrogen combustion can be represented as follows [12, 13]:

$$H_2 + O_2 \rightarrow 2OH^{\bullet}, \quad k_0 = 1.92 \times 10^{14}\exp(-21890/T)\ \text{cm}^3\,\text{molecule}^{-1}\,\text{s}^{-1}\ [13], \tag{0}$$

$$OH^{\bullet} + H_2 \rightarrow H_2O + H, \quad k_1 = 4.63 \times 10^{12}\exp(-2100/T)\ \text{cm}^3\,\text{molecule}^{-1}\,\text{s}^{-1}\ [14], \tag{I}$$

$$H + O_2 \rightarrow OH^{\bullet} + O, \quad k_2 = 1.99 \times 10^{14}\exp(-8460/T)\ \text{cm}^3\,\text{molecule}^{-1}\,\text{s}^{-1}\ [15], \tag{II}$$

$$O + H_2 \rightarrow OH^{\bullet} + H, \quad k_3 = 1.88 \times 10^{14}\exp(-6897/T)\ \text{cm}^3\,\text{molecule}^{-1}\,\text{s}^{-1}\ [16], \tag{III}$$

$$H + O_2 + M \rightarrow HO_2^{\bullet} + M, \quad k_4 = 6.47 \times 10^{15}\,(T/298)^{-0.8}\ \text{cm}^6\,\text{molecule}^{-2}\,\text{s}^{-1}\ [17], \tag{IV}$$

$$H + HO_2^{\bullet} \rightarrow 2OH^{\bullet}, \quad k_5 = 1.69 \times 10^{14}\exp(-440/T)\ \text{cm}^3\,\text{molecule}^{-1}\,\text{s}^{-1}\ [15], \tag{V}$$

$$H_2 + HO_2^{\bullet} \rightarrow H_2O_2 + H, \quad k_6 = 3 \times 10^{13}\exp(-14400/T)\ \text{cm}^3\,\text{molecule}^{-1}\,\text{s}^{-1}\ [15], \tag{VI}$$

$$OH^{\bullet} + O \rightarrow H + O_2, \quad k_7 = 9.29 \times 10^{12}\ \text{cm}^3\,\text{molecule}^{-1}\,\text{s}^{-1}\ [18], \tag{VII}$$

$$O + HO_2^{\bullet} \rightarrow OH^{\bullet} + O_2, \quad k_8 = 3.25 \times 10^{13}\ \text{cm}^3\,\text{molecule}^{-1}\,\text{s}^{-1}\ [15], \tag{VIII}$$

$$OH^{\bullet} + HO_2^{\bullet} \rightarrow H_2O + O_2, \quad k_9 = 2.89 \times 10^{13}\exp(250/T)\ \text{cm}^3\,\text{molecule}^{-1}\,\text{s}^{-1}\ [17], \tag{IX}$$

$$2HO_2^{\bullet} \rightarrow H_2O_2 + O_2, \quad k_{10} = 2 \times 10^{12}\ \text{cm}^3\,\text{molecule}^{-1}\,\text{s}^{-1}\ [19], \tag{X}$$

$$H_2O_2 + M \rightarrow 2OH^{\bullet} + M, \quad k_{11} = 1.3 \times 10^{17}\exp(-22750/T)\ \text{cm}^3\,\text{molecule}^{-1}\,\text{s}^{-1}\ [20], \tag{XI}$$

$$H + H + M \rightarrow H_2 + M, \quad k_{12} = 2.2 \times 10^{15}\ \text{cm}^6\,\text{molecule}^{-2}\,\text{s}^{-1}\ [17]. \tag{XII}$$

A two-dimensional planar problem was considered. The characteristic time and length scales were set as follows: $t_0 = 1/(k_1^0[H_2]_0)$ and $x_0 = y_0 = (D_3/k_1^0[H_2]_0)^{1/2}$, where $k_1^0 = 4.63 \times 10^{12}$ cm^3 molecule^{-1} s^{-1} is the preexponential factor of reaction (I) and D_3 is the H_2 diffusion coefficient. The dimensional time (τ), longitudinal coordinate (ξ), transverse coordinate (η), and reactant concentrations (Y_i) were defined as $\tau = t/t_0$, $\xi = x/x_0$, $\eta = y/y_0$, and $Y_i = [i\text{th component concentration}]/[H_2]_0$. The dimensionless rate constant K_p was defined for bimolecular and termolecular reactions in different ways. For a bimolecular reaction, $K_p = k_p/k_1^0$, where p is the reaction number ($p \neq 4, 12$). For a termolecular reaction, $K_p = k_p[H_2]_0/k_1^0$, where $p = 4, 12$. The dimensionless diffusion coefficients $\delta_0 = \delta_1 = \delta_2 = \delta_3 = 1$, δ_4, δ_5, and δ_6 ($\delta_i = D_i/D_3$, $i = 0$–6) for the hydrogen–air mixture refer to $OH^{\bullet}$, O, H, H_2, O_2, $HO_2^{\bullet}$, and H_2O_2, respectively.

The set of diffusion and kinetic equations in these dimensionless variables for the above mechanism appears as

$$\partial Y_0/\partial\tau = \partial_0\left(\partial^2 Y_0/\partial\xi^2 + \partial^2 Y_0/\partial\eta^2\right) + K_0Y_3Y_5 - K_1Y_0Y_3 + K_2Y_2Y_4 + K_3Y_1Y_3 + 2K_5Y_2Y_6 - K_7Y_0Y_1 + K_8Y_1Y_5 + 2K_{11}Y_6,$$

$$\partial Y_1/\partial\tau = \delta_1\left(\partial^2 Y_1/\partial\xi^2 + \partial^2 Y_1\eta^2\right) + K_2Y_2Y_4 - K_3Y_1Y_3 - K_7Y_0Y_1 - K_8Y_1Y_5,$$

$$\partial Y_2/\partial\tau = \delta_2\left(\partial^2 Y_2/\partial\xi^2 + \partial^2 Y_2\eta^2\right) + K_1Y_0Y_3 - K_2Y_2Y_4 + K_3Y_1Y_3 - K_4Y_2Y_5M - K_5Y_2Y_6 + K_6Y_3Y_6 + K_7Y_0Y_1,$$

$$\partial Y_3/\partial\tau = \left(\partial^2 Y_3/\partial\xi^2 + \partial^2 Y_3/\partial\eta^2\right) - K_0Y_3Y_5 - K_1Y_0Y_3 - K_3Y_1Y_3 - K_6Y_3Y_6 + K_{12}Y_2^2M, \tag{1}$$

$$\partial Y_5/\partial\tau = \delta_5\left(\partial^2 Y_5/\partial\xi^2 + \partial^2 Y_5/\partial\eta^2\right) - K_0Y_3Y_5 - K_2Y_2Y_4 - K_4Y_2Y_5M + K_7Y_0Y_1 + K_8Y_1Y_5 + K_9Y_0Y_6 + K_{10}Y_6^2,$$

$$\partial Y_6/\partial\tau = \delta_6\left(\partial^2 Y_6/\partial\xi^2 + \partial^2 Y_6/\partial\eta^2\right) + K_4Y_2Y_5M - K_5Y_2Y_6 + K_6Y_3Y_6 - K_8Y_1Y_5 - K_9Y_0Y_6 - K_{10}Y_6^2,$$

$$\partial Y_7/\partial\tau = \delta_7\left(\partial^2 Y_7/\partial\xi^2 + \partial^2 Y_7/\partial\eta^2\right) + K_6Y_3Y_6 + K_{10}Y_6^2 - K_{11}Y_7M,$$

$$\partial T/\partial\tau = \delta_4\left(\partial^2 T/\partial\xi^2 + \partial^2 T/\partial\eta^2\right) + 1/(C_p\rho)\sum_p\sum_{m,n} Q_pK_pY_mY_n.$$

The last equation in (1), in combination with the others, makes it possible to calculate the temperature dynamics in the reacting gas. Here, C_p is the weighted average heat capacity at constant pressure, 0.25 cal g^{-1} K^{-1} [21]; δ_7 is the dimensionless thermal diffusivity of the gas mixture, accepted to be approximately equal to $\delta_7 \approx \delta_3$; T is temperature (K); ρ is the density of the gas mixture (g/cm^3); and $M = P \times 10^{19}/T$, where P is the total pressure (Torr). The heats of elementary reactions (Q_p) and diffusion coefficients were taken from [22, 23]. A kinetic scheme with the same elementary reactions, rate constants, etc. was used in the calculation of the laminar hydrogen/air flame speed [24].

The subscripts m and n at the dimensionless reactant concentrations, which vary between 0 and 6, stand for $OH^{\bullet}$, O, H, H_2, O_2, $HO_2^{\bullet}$, and H_2O_2, respectively. The subscript p at the dimensionless rate constants $K_p = k_p/k_1^0$ varies between 0 and 12, and its values correspond to reaction numbers in the kinetic mechanism of hydrogen combustion.

For self-ignition, the set of equations (1) is subject to the following initial conditions:

$$0 < \xi < L_0, \quad 0 < \eta < L,$$
$$\tau = 0: \quad Y_i(0,\xi,\eta) = 0 \quad (i \neq 3,4),$$
$$Y_3(0,\xi,\eta) = f_{H_2}, \quad Y_4(0,\xi,\eta) = f_{O_2};$$
$$T(0,\xi,\eta) = 300\ \text{K}.$$

The boundary conditions are as follows: $T(0,\xi,\eta = L) = 1000$ K,

$$0 < \eta < L: \quad T(\tau,0,\eta) = 300\ \text{K}, \quad T(\tau,L_0,\eta) = 300\ \text{K}. \tag{2}$$

For the disappearance of active species in under conditions of diffusion- or kinetically controlled chain termination, we used Dirichlet and Neumann boundary conditions, respectively:

$$0 < \xi < L_0, \quad 0 < \eta < L, \quad Y_i(\tau,\xi,\eta) = 0$$
$$\text{(Dirichlet boundary conditions)}, \quad (i \neq 3,4);$$
$$0 < \xi < L_0, \quad (\partial Y_i(\tau,\xi,\eta)/\partial\eta)_L = 0 \quad (i = 3,4) \tag{3}$$
$$\text{or} \quad (\partial Y_i(\tau,\xi,\eta)/\partial\eta)_L = 0$$
$$\text{(Neumann boundary conditions)},$$

where L is the dimensionless distance between the middle plane of the channel and its surface, L_0 is the dimensional channel length, f is the dimensionless concentration of the initial components (H_2, O_2) in the mixture. The total pressure of the gas mixture was set to be 10 Torr for the reason that the ignition delay at this pressure under our experimental conditions is comparable with the heating time. It is, therefore, possible to pass from self-ignition on the surface to self-ignition in the bulk by slightly changing the control parameters. Note that, as the total pressure of the mixture is raised, the heating time lengthens and, accordingly, the probability of self-ignition being initiated near the reactor wall further increases.

Symmetry conditions are formulated for the middle plain of the channel ($\eta = 0$).

The set of equations (1) was solved via finite-difference approximation over a uniform Cartesian grid. A two-step scheme was used, which ensured the second order of approximation with respect to the spatial variable [25]. We used 1600 computation points along the coordinate ξ and 600 ones along the coordinate ξ. With the above-specified characteristic scales, this corresponded to a channel diameter of 3.2 cm and a channel length of 4.2 cm. The Laplace operator was approximated using a "cross" scheme. The boundary conditions at the reactor wall and symmetry plane were also approximated accurate to the second order. In doing this, partial derivatives with respect to time were approximated by one-sided differences. The step sizes along the spatial and temporal coordinates were set so that, as they were further diminished, the solution of the problem did not change. Integration was carried out via an explicit scheme using the predictor–corrector procedure.

Figures 3–5 show the concentration profiles of intermediates calculated for the self-ignition of the stoichiometric $2H_2 + O_2$ mixture at the points in time at which the reactive intermediate concentrations change sharply. The gray tones in Fig. 1 represent the spatial distribution of the concentrations Y_i. The boundaries between tones are concentration isolines. The darker color means a higher concentration between the concentration isolines. The interval between two concentration isolines corresponds to a 30% change in the concentration. In each of these two-dimensional distribution patterns (Figs. 3–5), the top of the "frame" corresponds to the channel wall and the bottom of the "frame" corresponds to the middle plane. The gas temperature uniformity is qualitatively characterized by the temperature difference between the center of the reactor and the hot wall. The time dependence of the channel middle temperature in the time interval $0 < \tau < \tau_{fig}$ (curve) and the hot wall temperature (straight line) are plotted in Figs. 3–5 against the black background. The merging of the curve and the straight line means that a uniform temperature distribution is established up to the middle of the channel. Here, τ_{fig} is the onset time of the intensive chemical reaction for the given variant of calculation and, at the same time, the instant the frame was obtained. In our calculations, the onset time of the intensive chemical reaction was taken to coincide with the instant the concentration of some reactive species exceeded a certain threshold value. For $HO_2^{\bullet}$, this threshold was 10^{-3} in dimensionless units.

With the Dirichlet and Neumann boundary conditions, we were able to qualitatively estimate the effects of the reactive species generation and heterogeneous disappearance rates on the spatial development of chain self-ignition. Figure 3 illustrates the spatial distributions of the reactive species H, O, $OH^{\bullet}$, and $HO_2^{\bullet}$ at the onset of the intensive, kinetically controlled chemical reaction ($(\partial Y_i(\tau,\xi,\eta)/\partial\eta)_L = 0\,(i = 3,4)$; Neumann boundary conditions) for various rates of chain initiation (reaction (0)). The rate of this reaction was varied by changing its activation energy. According to Baulch et al. [18], $E_0/R = 24500$ K. However, as was demonstrated by our calculations, the hydrogen–oxygen mixture ignites in the bulk at a smaller value of $E_0/R = 18000$ K. For this reason, our calculations were limited to the 2000 K $< E_0/R <$ 20000 K range.

Reducing E_0/R from 20000 to 12000 K exerts a strong effect on the onset time of the intensive chemical reaction (Fig. 3): the dimensionless onset time decreases from 1800 to 170. It is also clear from Fig. 3 that, at $E_0/R = 12000$ K, self-ignition begins on the reactor surface because the gas temperature in the middle of the channel is much lower than the temperature of the hot wall. As E_0/R is raised, the gas is heated

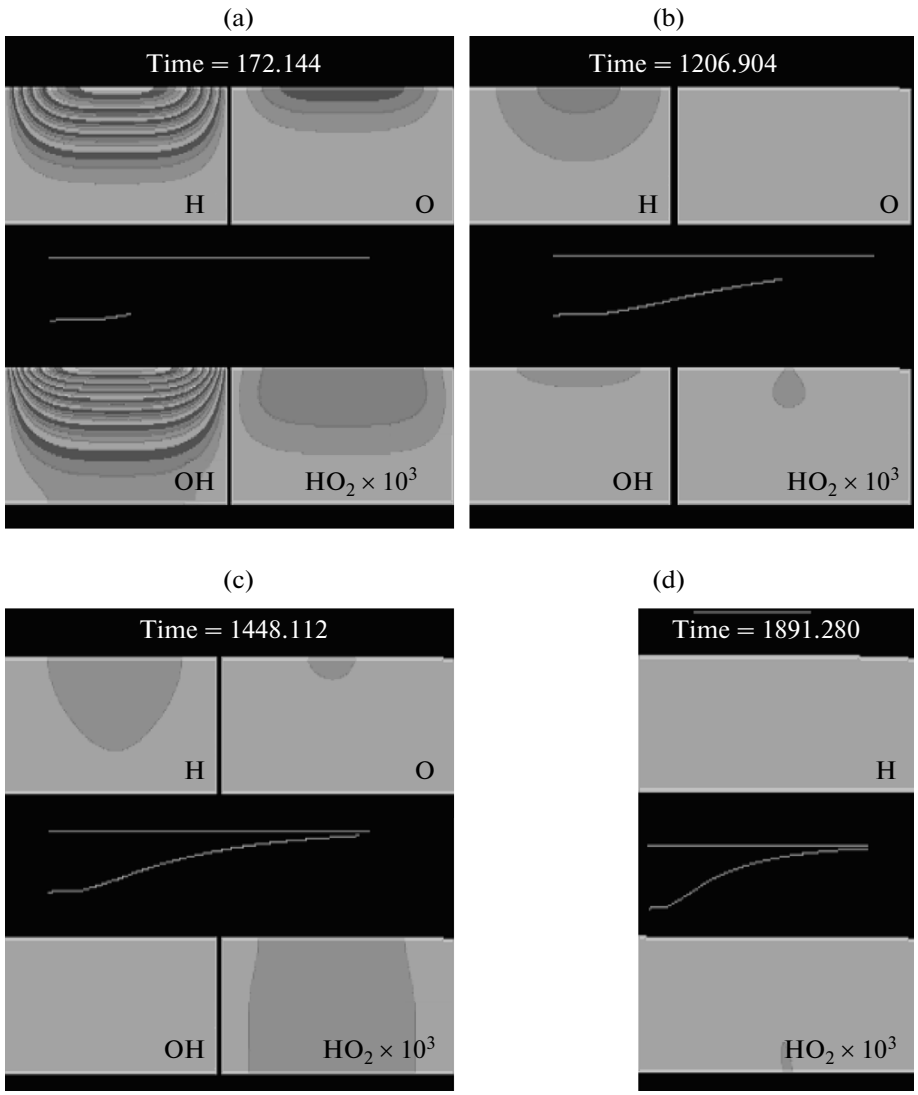

Fig. 3. Simulation of the self-ignition of the $2H_2 + O_2$ mixture in the kinetically controlled region of chain termination. $T_0 =$ 1000 K; $P = 10$ Torr; $-E_0/R =$ (a) 12000, (b) 16500, (c) 18000, and (d) 20000 K. The straight line is the wall temperature, and the curve is the gas temperature in the center of the reactor. At the points in time indicated in the panels, $[HO_2^{\bullet}] = 10^{-3}$ (in dimensional units).

progressively more uniformly and self-ignition becomes more uniform across the reactor. For example, self-ignition at $E_0/R = 20000$ K begins in the central zone of the reactor because the gas temperature in the middle of the channel becomes equal to the temperature of the hot wall sooner than an ignition event takes place. Thus, the results of numerical simulation displayed in Fig. 3 illustrate the observations presented in Fig. 1, specifically, the fact that, in the kinetically controlled region of chain termination, an increase in the chain initiation rate can generate a primary self-ignition area near the channel surface.

Figures 4a and 4b show the spatial distributions of the reactive species H, O, $OH^{\bullet}$, and $HO_2^{\bullet}$ at the onset of the intensive, kinetically controlled chemical reaction ($(Y_i(\tau,\xi,L) = 0 (i = 3,4)$; Neumann boundary conditions), again for various rates of chain initiation (reaction (0)). As E_0/R is decreased from 18000 to 12000 K, the dimensionless onset time of the intensive chemical reaction decreases from 1100 to 320 (Fig. 4). It is also clear from Fig. 4 that, as E_0/R is raised, self-ignition becomes more uniform across the reactor and an E_0/R value of 18000 K ensures the appearance of a primary self-ignition area in the middle of the channel (Fig. 4c) owing to the change in the ratio of the heating time to the characteristic time of the chemical reaction. These calculations suggest that a transition to uniform self-ignition can be expected in those experiments under diffusion-controlled chain termination

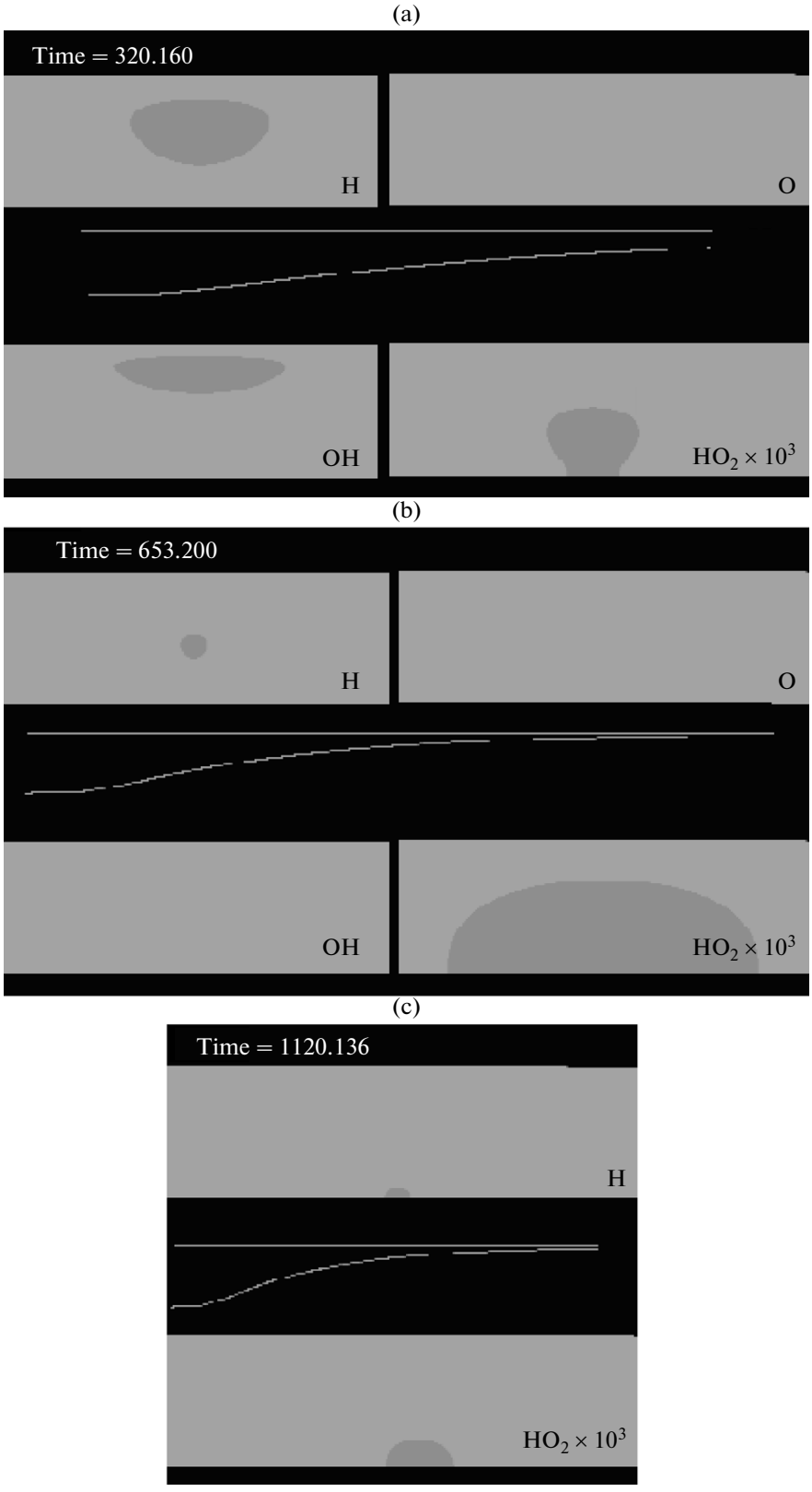

Fig. 4. Simulation of the self-ignition of the $2H_2 + O_2$ mixture in the diffusion-controlled region of chain termination. $T_0 =$ 1000 K; $P = 10$ Torr; $-E_0/R =$ (a) 12000, (b) 15000, and (c) 18000 K. The straight line and curve against the black background are the wall temperature and the gas temperature in the center of the reactor, respectively. At the points in time indicated in the panels, $[HO_2^{\bullet}] = 10^{-3}$ (in dimensional units).

conditions in which the heating time is much shorter than the induction period (Fig. 1c).

Figures 5a and 5b present the results of the numerical simulation of the spatial development of self-ignition in the $2H_2 + O_2$ mixture under diffusion-controlled chain termination conditions for $OH^{\bullet}$, O, and $HO_2^{\bullet}$ reactive species in the case of the existence of a flux of hydrogen atoms generated by the surface into the bulk. This flux was set to be 10^{-7} in dimensionless units ($k_0[H_2]_0[O_2]_0/k_1[H_2]_0$, where $k_0 = 10^{-19}$ cm^3 mol^{-1} s^{-1}). Two successive "frames" are shown, which pertain to the very onset of self-ignition at $E_0/R = 18000$ K. Clearly, the active species flux from the surface to the bulk leads to the nonuniform development of self-ignition in the reactor space. Note that space self-ignition occurs at the same values of the determining parameters, but in the absence of a hydrogen atom flux into the bulk (Fig. 4c). It is likely that the same situation takes place in the self-ignition of hydrocarbons over a quartz surface and in hydrogen ignition over a fresh quartz surface (Figs. 1, 2).

Our experiments and calculations demonstrate that the uniformity of self-ignition in the reactor space depends on the self-ignition time at the hot wall temperature to the reaction space heating time. In addition, the uniformity of self-ignition for branched-chain processes depends on the properties of the surface [26]. The nonuniformity of self-ignition shows itself most clearly at a high chain initiation rate. With an increasing rate of generation of reactive species by the surface or with an increasing total pressure of the combustible mixture (which lengthens the heating time), the self-ignition problem transforms into the problem of mixture ignition by the hot wall, which can also catalyze the chemical reaction. The results of this study should be taken into consideration in the interpretation of experimental data on self-ignition at elevated pressures, including at the third limit of hydrogen oxidation [2], because, when there is a heating stage, thermal explosion and ignition are characterized by different dependences of the ignition time on the dimensions of the reactor [27].

Thus, using high-speed color cinematography, we studied the spatial development of chain self-ignition in the oxidation of stoichiometric mixtures of hydrogen, methane, and isobutylene with oxygen at total pressures of 10–100 Torr and $T = 750$–1000 K. It was found that the spatial development of self-ignition (surface versus space ignition) in the case of the branched-chain mechanism of the chemical reaction is governed by the ratio of the reaction time at the hot wall temperature to the heating time of the combustible mixture and by the properties of the reactor surface. It was demonstrated using numerical simulation that, by varying the activation energy of the chain initiation reaction, it is possible a transition from space ignition to surface ignition both for diffusion-controlled and kinetically controlled chain termination on the reactor surface. A flux of reactive species from the surface to the bulk leads to the nonuniform development of self-ignition in the reactor space. The calculated and experimental data are in qualitative agreement.

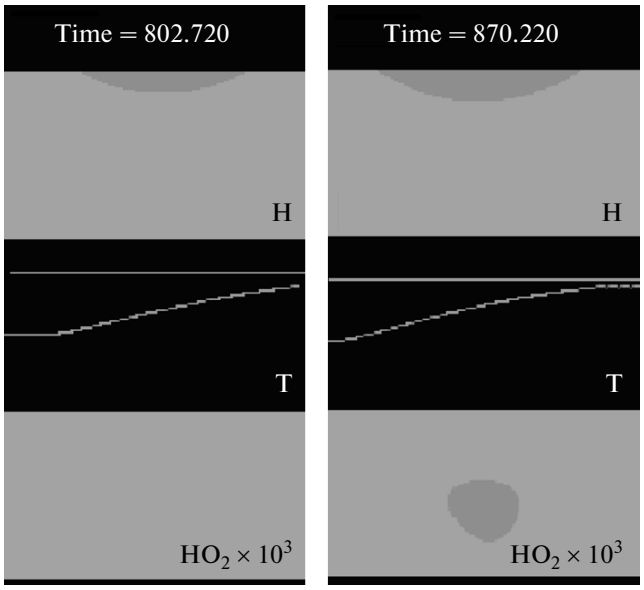

Fig. 5. Simulation of the development of self-ignition in the $2H_2 + O_2$ mixture in the diffusion-controlled region of chain termination for $OH^{\bullet}$, O, and $HO_2^{\bullet}$ in the presence of a flux of surface-generated H atoms into the bulk. $T_0 = 1000$ K; $P = 10$ Torr. The straight line and curve against the black background are the wall temperature and the gas temperature in the center of the reactor, respectively. At the points in time indicated in the panels, $[HO_2^{\bullet}] = 10^{-3}$ (in dimensional units).

ACKNOWLEDGMENTS

The authors are grateful to V.V. Azatyan, Corresponding Member of the Russian Academy of Science, for helpful remarks.

This work was supported by the Russian Foundation for Basic Research, grant nos. 08-03-01034-a, 10-08-00305-a, and 09-03-00622-a.

REFERENCES

1. Karpov, V.P., Rubtsov, N.M., Ryzhkov, O.T., Temchin, S.M., and Chernysh, V.I., *Khim. Fiz.*, 1998, vol. 17, no. 4, p. 73.
2. Semenov, N.N., *O nekotorykh problemakh khimicheskoi kinetiki i reaktsionnoi sposobnosti* (Topics in Chemical Kinetics and Reactivity), Moscow: Akad. Nauk SSSR, 1958.
3. Zel'dovich, Ya.B., Barenblatt, G.A., Librovich, V.B., and Makhviladze, D.V., *Matematicheskaya teoriya rasprostraneniya plameni* (Mathematical Theory of Flame Propagation), Moscow: Akad. Nauk SSSR, 1980.

4. Frank-Kamenetskii, D.A., *Diffuziya i teploperedacha v khimicheskoi kinetike* (Diffusion and Heat Transfer in Chemical Kinetics), Moscow: Nauka, 1967.
5. Merzhanov, A.G. and Khaikin, B.I., *Teoriya voln goreniya v gomogennykh sredakh* (Theory of Combustion Waves in Homogeneous media), Chernogolovka, Moscow oblast: Inst. of Structural Macrokinetics and Materials Science, 1992.
6. Azatyan, V.V., Pyatnitskii, Yu.I., Boldyreva, N.A., and Shaprinskaya, T.M., *Khim. Fiz.*, 1988, vol. 7, no. 2, p. 235.
7. Azatyan, V.V., *Zh. Fiz. Khim.*, 1998, vol. 72, no. 3, p. 391 [*Russ. J. Phys. Chem.* (Engl. Transl.), vol. 72, no. 3, p. 319].
8. Azatyan, V.V., Rubtsov, N.M., Ryzhkov, O.T., and Chernysh, V.I., *Kinet. Katal.*, 1996, vol. 37, no. 6, p. 805 [*Kinet. Catal.* (Engl. Transl.), vol. 37, no. 6, p. 747].
9. Lewis, B. and von Elbe G., *Combustion, Explosions and Flame in Gases*, New York: Academic, 1987.
10. Rubtsov, N.M., Tsvetkov, G.I., and Chernysh, V.I., *Kinet. Katal.*, 2008, vol. 49, no. 3, p. 363 [*Kinet. Catal.* (Engl. Transl.), vol. 49, no. 3, p. 344].
11. Neiman, M.B. and Egorov, L.N., *Zh. Fiz. Khim.*, 1932, vol. 3, no. 1, p. 61.
12. Aghalayam, P., Bui, P.-A., and Vlachos, D.G., *Combust. Theory Model.*, 1998, vol. 2, p. 515.
13. Azatyan, V.V., Bolod'yan, I.A., Navtsenya, V.Yu., and Shebeko, Yu.N., *Zh. Fiz. Khim.*, 2002, vol. 76, no. 5, p. 775 [*Russ. J. Phys. Chem.* (Engl. Transl.), vol. 76, no. 5, p. 677].
14. Azatyan, V.V., Aleksandrov, E.N., and Troshin, A.F., *Kinet. Katal.*, 1975, vol. 16, no. 2, p. 306.
15. Atkinson, R., Baulch, D.L., Cox, R.A., Hampson, R.F., Jr., Kerr, J.A., Rossi, M.J., and Troe, J., *J. Phys. Chem. Ref. Data*, 1997, vol. 26, p. 1329.
16. Baulch, D.L., Cobos, C.J., Cox, R.A., Esser, C., Frank, P., Just, Th., Kerr, J.A., Pilling, M.J., Troe, J., Walker, R.W., and Warnatz, J., *J. Phys. Chem. Ref. Data*, 1992, vol. 21, p. 411.
17. Ryu, S.-O., Hwang, S.M., and Rabinowitz, M.J., *Chem. Phys. Lett.*, 1995, vol. 242, p. 279.
18. Baulch, D.L., Bowman, C.T., Cobos, C.J., Cox, R.A., Just, Th., Kerr, J.A., Pilling, M.J., Stocker, D., Troe, J., Tsang, W., Walker, R.W., and Warnatz, J., *J. Phys. Chem. Ref. Data*, 2005, vol. 34, p. 566.
19. Yang, H., Gardiner, W.C., Shin, K.S., and Fujii, N., *Chem. Phys. Lett.*, 1994, vol. 231, p. 449.
20. Park, Y.K. and Vlachos, D.G., *J. Chem. Soc., Faraday Trans.*, 1998, vol. 94, p. 735.
21. *Tablitsy fizicheskikh velichin: Spravochnik* (Tables of Physical Quantities: A Handbook), Kikoin, E.K., Ed., Moscow: Atomizdat, 1976.
22. Hitch, B.D. and Senser, D.W., *26th Aerospace Sciences Meeting*, Reno, Nev., 1988, AIAA-1988-732.
23. Konnov, A.A., *Khim. Fiz.*, 2004, vol. 23, no. 1, p. 5.
24. Rubtsov, N.M., Seplyarskii, B.S., Chernysh, V.I., and Tsvetkov, G.I., *Mendeleev Commun.*, 2008, vol. 18, p. 1.
25. Marchuk, G.I., *Metody vychislitel'noi matematiki* (Methods of Computational Mathematics), Moscow: Nauka. 1989.
26. Azatyan, V.V., *Usp. Khim.*, 1985, vol. 33, no. 1, p. 33.
27. Merzhanov, A.G., Abramov, V.G., and Gontkovskaya, V.T., *Dokl. Akad. Nauk SSSR*, 1963, vol. 148, no. 1, p. 156.